Am J Transl Res 2026;18(3):2548-2559
www.ajtr.org /ISSN:1943-8141/AJTR0170728

Original Article

Study on the protective effects and molecular mechanisms of L-sodium lactate in mouse colitis

Pan Huang[1,2*], Kang-Ping Shao[2*], Si-Yu Wang[2,3], Gen-Bao Shao[1,2], Jian-Peng Hu[1], Zheng-Rong Zhou[2]

[1]Institute of Urinary System Diseases, The Affiliated People's Hospital, Jiangsu University, Zhenjiang 212002, Jiangsu, PR China; [2]School of Medicine, Jiangsu University, Zhenjiang 212013, Jiangsu, PR China; [3]Chongqing Hospital, Union Hospital, Tongji Medical College, Huazhong University of Science and Technology, Chongqing 401121, PR China. [*]Equal contributors.

Received December 14, 2025; Accepted February 9, 2026; Epub March 15, 2026; Published March 30, 2026

Abstract: The present study investigates the therapeutic potential of L-sodium lactate in a dextran sodium sulfate (DSS)-induced colitis C57BL/6J mice model. Treatment with L-sodium lactate significantly mitigated disease severity, as evidenced by reduced colon shortening ($P < 0.05$) and elevated levels of the anti-inflammatory cytokine IL-10 ($P < 0.05$). Tandem mass tag (TMT)-based proteomic profiling revealed dual mechanisms, involving the up-regulation of cell cycle- and proliferation-associated proteins (PCNA, SMC, eEF2K) and the down-regulation of immune-related proteins (immunoglobulin variants, Granzyme A). *In vitro*, 10 μM L-sodium lactate has been demonstrated to promote the proliferation and migration of colorectal cancer cells (MC38/HCT116) ($P < 0.05$), accompanied by increased expression of c-Myc and PCNA. Collectively, these findings suggest that L-sodium lactate may enhance mucosal repair while suppressing histopathological injury in colitis, although further studies are needed to confirm these mechanisms.

Keywords: L-sodium lactate, colitis, proteomics, cell proliferation

Introduction

Inflammatory bowel disease (IBD) is a complex disorder of unknown cause, affecting about 14.3 per 100,000 people, and is increasingly common in young individuals in East Asia, including China [1, 2]. IBD has been demonstrated to result in severe inflammatory responses and tissue damage, thus establishing itself as a significant risk factor for colorectal cancer [3, 4]. The disease progression of IBD is influenced by a variety of factors, including genetic susceptibility, environmental triggers, and changes in the gut microbiome [5-7]. In this complex microenvironment, microbial and host-derived metabolites have been identified as critical mediators that can significantly influence intestinal homeostasis and inflammatory processes [8-10].

A significant metabolic characteristic of the inflamed IBD gut is the accumulation of lactate, which is a primary outcome of anaerobic glycolysis [11]. Lactate exists in two enantiomeric forms: L-lactate and D-lactate exhibit divergent metabolic fates and biological activities [12]. It is crucial to note that mammalian metabolism demonstrates a pronounced predilection for the L-isomer [13]. Most mammals, including humans and rodents, abundantly express L-lactate dehydrogenase (L-LDH). This enzyme catalyzes the conversion of L-lactate into pyruvate for entry into the tricarboxylic acid (TCA) cycle [14, 15]. In contrast, they exhibit a lack of an analogous, highly active D-lactate dehydrogenase (D-LDH), resulting in inefficient D-lactate metabolism and the potential accumulation of D-lactate. Accumulated D-lactate has been associated with metabolic acidosis and neurotoxicity in specific pathological conditions [16-18]. Recent studies have indicated that L-sodium lactate has antioxidant and immunomodulatory properties, and may affect the development of conditions such as metabolic syndrome, diabetes and cardiovascular disease by influencing metabolic pathways [19-22]. Therefore, this study specifically focuses on L-lactate to investigate its physiological role in IBD.

https://doi.org/10.62347/FDGK6829

Material and methods

Laboratory mice for animal experiments

The Center of Animal Laboratory at Jiangsu University (Jiangsu, China) provided male C57BL/6J mice with an age range of 6-8 weeks. The mice were acclimatized to a pathogen-free laboratory environment maintained at 22±3°C with 40-60% humidity. The mice were provided with food and water ad libitum. To minimize potential confounders, cages were randomly repositioned on the rack daily throughout the experiment to account for any environmental gradients (e.g., light, temperature, or human traffic). All experimental protocols involving animals received approval from the Animal Ethics Committee of Jiangsu University (Approval No.: UJS-IACUC-2025022101) and were conducted in accordance with the university's guidelines for the care and use of laboratory animals.

IBD model establishment

The mice were randomly assigned to two groups: DSS-induced IBD group (DSS, n = 12) and DSS-induced IBD group with L-sodium lactate treatment (LAC, n = 12). The animals were housed in groups within ventilated cages, with a maximum of five mice permitted per cage. The investigator who performed the animal allocation and daily treatments was necessarily aware of the group identities. However, the researchers tasked with evaluating the outcomes and conducting the statistical analysis were unaware of the group allocation throughout the process. Subsequent to a three-day acclimatization period, the mice in the LAC group were administered 30 mM L-sodium lactate before the establishment of the IBD model. Both groups were subjected to a 7-day regimen of 2% DSS in drinking water to induce intestinal inflammation. Concurrently, the LAC group received L-sodium lactate in their drinking water throughout the DSS-induced colitic period.

Colon collection and inflammatory cytokine detection

All mice were anesthetized using pentobarbital (40 mg/kg), and approximately 500 μL of blood was collected via orbital puncture. Subsequently, the mice were euthanized by carbon dioxide (30-70%) asphyxiation. If the mice exhibited no movement, no breathing, and dilated pupils, the carbon dioxide valve was turned off and the mice were observed for an additional 2-3 min to confirm their deaths. During the course of the experimental period, no unexpected adverse events related to the L-sodium lactate treatment or the DSS model were observed. Blood was collected, and serum was separated after centrifugation at 3,000 rpm for 15 minutes at 4°C. Colon tissues were measured and stored in a freezer (-80°C). The concentrations of cytokines, such as IL-6 and IL-10 as well as lactate were measured in the serum using commercial enzyme-linked immunosorbent assay (ELISA) kits (all purchased from Jianglai Biotech, Shanghai, China) according to the manufacturer's protocols [23].

Tandem mass tag (TMT)-based quantitative proteomics analysis

The TMT technology is a quantitative labelling method in proteomics that facilitates the simultaneous comparison of protein expression levels across multiple samples in a single experiment [24-26]. This approach enables the identification of differentially expressed proteins (DEPs) in a range of biological processes and diseases. It is imperative for the prediction of therapeutic targets and the elucidation of the potential mechanisms of drug action [27, 28].

Colon protein extraction

In order to reduce individual differences, six colon tissue samples were collected per group, of which five were randomly selected for proteomic analysis to ensure statistical robustness. Samples taken from the colon tissue were transferred into centrifugal tubes (2 mL). Next, we added 1X Roche cocktail at final concentration, lysis solution comprising 8M Urea/50 mM Tris-hydrochloric acid (HCl) and steel balls into the tubes. The sample was then ground into fine powder on ice. To obtain a 10 mM final concentration, we collected the supernatant before adding dithiothreitol (DTT) after centrifugation (20,000×g, 4°C) for 15 minutes. Subsequently, the mixture was placed in water baths at 37°C for a duration of one hour prior to the addition of iodoacetic acid (IAA) to achieve a final concentration of 20 mM. Later, the tubes were placed in the dark for 30 min. The Bradford method was utilized to ascertain the protein concentration prior to detection via sodium

dodecyl sulphate polyacrylamide gel electrophoresis [29].

Protein digestion and labeling

Prior to vacuum drying of the sample, the protein solution underwent hydrolysis with trypsin, and desalting with Waters solid-phase extraction cartridges. Next, the digested peptides were redissolved in 30 μL aliquots of 100 mM triethylammonium bicarbonate (TEAB). The peptides were then labelled with the TMTpro-16plex reagent for a period of 1-2 hours. The labeling reaction was performed by dissolving the reagent in 100% anhydrous acetonitrile.

High pH reverse-phase separation

In order to execute this separation, the peptides from each sample (in equal amounts) were combined and subsequently diluted with solvent A (pH 9.8, 5% ACN) prior to column injection. The peptide mixture was subjected to fractionation by means of an Agilent ZORBAX 300-Extend-C18 column in combination with a Thermo-Scientific UltiMate™ 3000-Binary Rapid Separation System. Subsequently, gradient elution was performed at a flow rate of 0.3 mL/min, with a transition time of 38 minutes from 5% to 21% of solvent B (pH 9.8, 97% ACN). Also, the gradient was increased over 20 minutes to solvent B (40%) and in 2 minutes to solvent B (90%), maintaining for another 3 minutes with solvent B (90%), then equilibrating for 10 minutes with solvent B (5%). At 214 nm, the elution peaks were monitored and the fractions collected at one-minute intervals. The fractions were then combined on the basis of the corresponding chromatograms.

Identification and quantitation of proteins

The TMT-plexed MS/MS raw data was analyzed using MaxQuant (version 2.1.4.0) software. Related parameters and instructions are as follows: Max missed cleavages: 2; Peptide mass tolerance: ± 20 ppm; Fragment mass tolerance: 0.05 Da; Peptide false discovery rate (FDR): ≤ 0.01; Protein quantification: the protein ratios were calculated as the median of only unique peptides of the protein.

Bioinformatics and data analysis

R software (version 4.0.0) was utilized to conduct the statistical analysis. The (medium) method was employed for the normalization of raw protein intensity data. In addition, the metaX package was employed to perform the principal component analysis (PCA), while the pheatmap package was utilized for the purpose of hierarchical clustering. To identify the DEPs, we applied a facilitated t-test statistic differential analysis, wherein a significant threshold of *fold change (FC)* > 1.2 (or < 0.83) and $P < 0.05$ (T-test) were used [30]. To annotate protein sequences individually, we conducted hypergeometric-based enrichment analyses for Gene Ontology (GO), Reactome and Kyoto Encyclopedia of Genes and Genomes (KEGG) pathways. The transcription factor annotation was performed based on the Animal TFDB and Plant TFDB databases. In addition, the WoLF PSORT tool was utilized to determine the subcellular localization of the transcription factors. The mass spectrometry proteomics data have been deposited to the ProteomeXchange Consortium (https://proteomecentral.proteomexchange.org) via the iProX partner [31, 32] repository with the dataset identifier PXD069291.

Cell culture and treatment

The human colorectal carcinoma cell line HCT-116 (BC-C-HU-054) and the mouse colon carcinoma cell line MC38 (BC-C-MI-011) were obtained from Nanjing Senbio Biotechnology Co., Ltd. (China). The MC38 murine colon adenocarcinoma cells and HCT116 human colorectal carcinoma cells were maintained in Dulbecco's modified Eagle medium (DMEM) with the following supplements: 10% fetal bovine serum (FBS) and 1% penicillin/streptomycin. The cells were cultivated at 37°C in a humidified 5% CO_2 atmosphere. The cells were divided into three treatment groups: Ctrl group: culture medium without L-sodium lactate supplementation; Low-dose group: medium containing 10 μM L-sodium lactate; High-dose group: medium containing 100 μM L-sodium lactate.

Cell proliferation assay

The assessment of cell viability was conducted through the implementation of an assay of Cell Counting Kit-8 (CCK-8). In summary, 5×10^3 cells/well were seeded in 96-well plates. Following a 24-hour attachment period, the cells were subjected to treatment with the respective concentrations of L-sodium lactate for a further 24 hours. The CCK-8 reagent (10

μL/well) was added 2 hours prior to measurement, and the resulting optical density was measured at a wavelength of 450 nm using a microplate reader.

Colony formation assay

The Cells (500/well) were plated in 6-well plates and cultured for 10-14 days with medium renewal every 2 days. The colonies were fixed with 4% paraformaldehyde, stained with 0.1% crystal violet, and enumerated under microscopy.

Wound healing assay

Confluent monolayers in 6-well plates were scratched using a 200 μL sterile pipette tip. After PBS washing, fresh media containing L-sodium lactate were added. Migration distance was quantified at 24 h.

Western blot analysis

Subsequent mechanistic investigations (Western blotting) were performed exclusively with 10 μM treatment, with the objective of focusing on the active dose. Total proteins were extracted using RIPA buffer supplemented with protease inhibitors. Thirty μg protein/lane was separated by SDS-PAGE and transferred to polyvinylidene fluoride (PVDF) membranes. Following blocking with 5% non-fat milk, membranes were incubated with primary antibodies (see Table S1 for details) overnight at 4°C, followed by HRP-conjugated secondary antibodies. Protein bands were visualized using an enhanced chemiluminescence (ECL) substrate and subsequently quantified by means of Image Lab software.

Statistical analysis

All experiments were performed in triplicate with at least three biological replicates. The analysis of the data was conducted using GraphPad Prism software, version 8.0, with statistical significance defined as $P < 0.05$. Data are presented as mean ± SD. Comparisons between the two groups were performed using Student's t-test; comparisons among three or more groups were analyzed by one-way ANOVA followed by Tukey's post hoc test. A P value < 0.05 was considered statistically significant. Significance is denoted as follows: $*P < 0.05$, $**P < 0.01$, $***P < 0.001$.

Results

L-sodium lactate alleviates DSS-induced mouse colitis

As shown in **Figure 1A-C**, the LAC group showed significantly preserved colon length ($P < 0.05$), but no significant difference in body weight changes ($P > 0.05$) was observed. Similarly, no significant differences were observed in serum IL-6 levels or L-sodium lactate levels in serum and fecal samples between the two groups ($P > 0.05$). However, compared with the DSS group, the LAC group exhibited a significant increase in serum IL-10 levels ($P < 0.05$, **Figure 1D-G**).

Effects of L-sodium lactate on proteomic profiles in mouse colitis

PCA and three-dimensional PCA plots were generated based on the expression levels of reliably identified proteins. These visualizations, which portray the sample differences and groupings across various dimensions, indicated that samples consistently cluster within their respective groups, thus suggesting stable data with high reproducibility (**Figure 2A**, **2B**). Further analysis, including Box, Coefficient of Variance and Correlation Plots of the protein expression levels revealed minimal sample variation and concentrated data distribution (**Figure 2C**, **2D**). To discern significant DEPs between the DSS and LAC groups in mouse intestinal tissue samples, we utilized TMT labeling coupled with quantitative proteomics for an in-depth comparative analysis. Through analysis of data from 5 samples per group, we generated a volcano plot to delineate the DEPs (**Figure 2E**, **2F**). The plot presents the FC in protein expression on the horizontal axis and the negative logarithm *(-log10)* transformed Q-values on the vertical axis, thus offering a graphical depiction of the relative protein abundance and statistical significance of DEPs between the two groups.

As depicted, the DEPs were classified into three distinct categories, namely up-regulated, down-regulated, and unchanged. The tables present the top 10 up-regulated proteins (**Table 1**) and the top 10 down-regulated proteins (**Table 2**). Among the top 10 up-regulated DEPs, Proliferating Cell Nuclear Antigen (PCNA), Structural

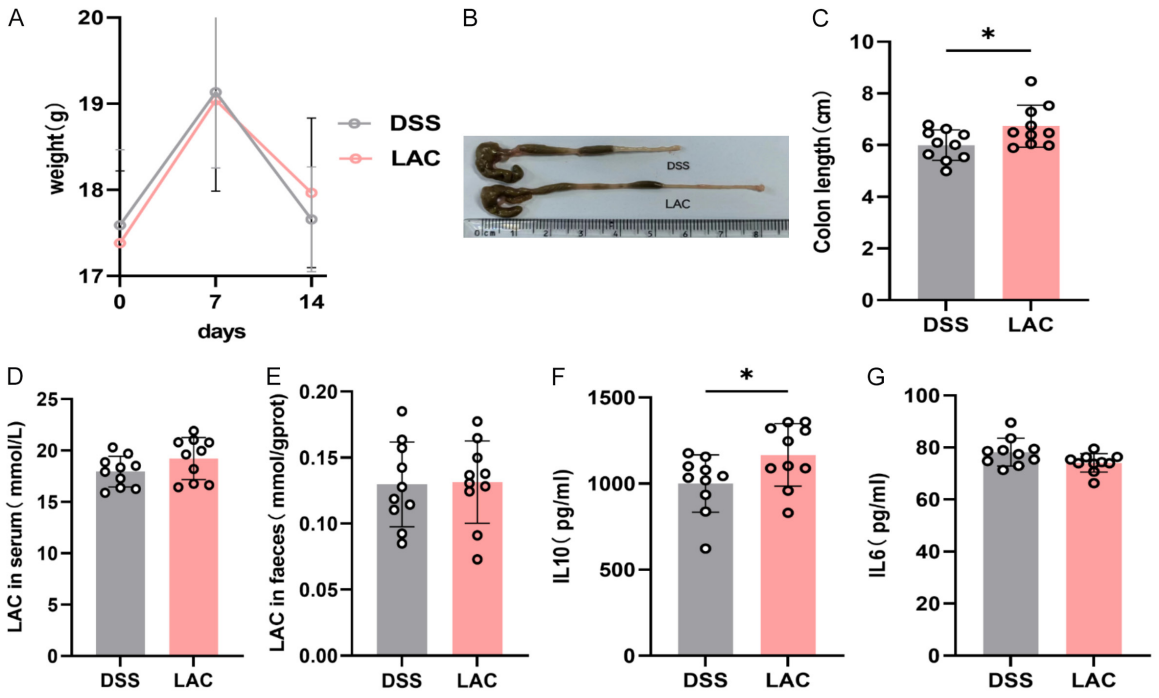

Figure 1. Effects of L-sodium lactate on DSS-induced colitis in mice. A: Body weight changes; B: Mice colons; C: Colon length changes; D: Serum lactate concentrations; E: Fecal lactate concentrations; F: Serum interleukin (IL)-6 concentrations; G: Serum IL-10 concentrations (N = 10). *P < 0.05, **P < 0.01, ***P < 0.001.

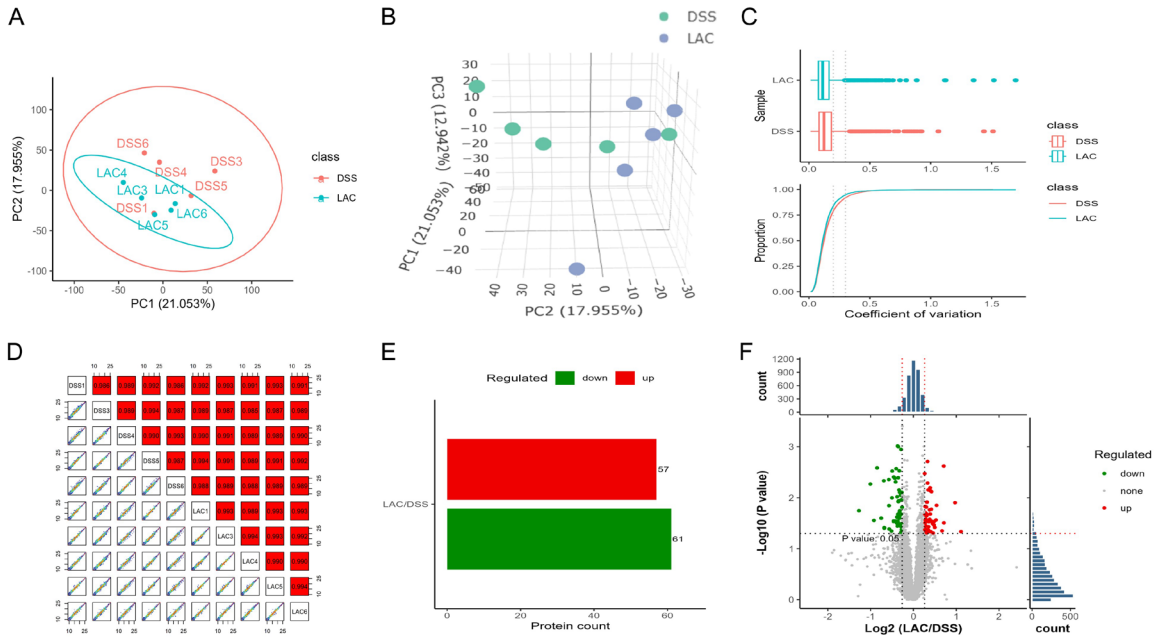

Figure 2. Identification and quantitative analysis of proteins. A: Principal component analysis (PCA) of samples; B: 3D-PCA of samples; C: Box and coefficient of variance plot; D: Correlation chart; E: The number of DEPs in down-regulated and up-regulated proteins; F: Volcano plot depicting fold change (FC) and significance distribution of discovered proteins among LAC and DSS groups, the respective red and green spots point substantially up-regulated down-regulated proteins.

Maintenance of Chromosomes protein (SMC), and Eukaryotic Elongation Factor 2 Kinase (eEF2K) play a crucial role in cell cycle regulation. Ten down-regulated DEPs are predomi-

Table 1. Up-regulation of the top 10 DEPs

Gene name	Protein description	*P* Value	FC	Regulation
Mfn1	Mitofusin-1 (Fragment)	0.008187644	1.292049622	Up
Anp32e	Acidic leucine-rich nuclear phosphoprotein 32 family member E	0.01917105	1.280510717	Up
Pex26	Peroxisome assembly protein 26	0.022396727	1.326933476	Up
Tnnc2	Troponin C, skeletal muscle	0.022677003	1.302264303	Up
Smc4	Structural maintenance of chromosomes protein	0.026015512	1.253675357	Up
Eef2k	Eukaryotic elongation factor 2 kinase (Fragment)	0.026372908	1.289915105	Up
Pcna	Proliferating cell nuclear antigen	0.030750996	1.260719623	Up
Flg	Filaggrin	0.0352016	1.871122181	Up
Ptprn2	Receptor-type tyrosine-protein phosphatase N2	0.035495379	1.327532197	Up
Dok3	Docking protein 3	0.036024451	1.274523213	Up

Table 2. Down-regulation of the top 10 DEPs

Gene name	Protein description	*P* Value	FC	Regulation
Igkv5-39	Immunoglobulin kappa variable 5-39	0.00071	0.599505	Down
Igkv8-21	Immunoglobulin kappa variable 8-21 (Fragment)	0.001029	0.585261	Down
Nr3c1	Glucocorticoid receptor	0.001218	0.803666	Down
Fkbp5	Peptidyl-prolyl cis-trans isomerase FKBP5	0.001606	0.771748	Down
Igkv8-19	Immunoglobulin kappa variable 8-19	0.002969	0.634631	Down
Slc44a4	Choline transporter-like protein	0.003038	0.73684	Down
B3galt5	Beta-1,3-galactosyltransferase 5	0.003368	0.755554	Down
Ighv9-4	Immunoglobulin heavy variable 9-4	0.004068	0.408272	Down
Tspan8	Tetraspanin-8	0.005438	0.731221	Down
Gzma	Granzyme A	0.00704	0.566982	Down

nantly implicated in immune modulation, cellular signal transduction, and metabolic regulation, among other biological processes.

In addition, to investigate into the relational patterns among DEPs between DSS and LAC groups, we performed hierarchical clustering analysis and constructed a heatmap depicting the DEPs (**Figure 3B**). Subsequently, we conducted GO enrichment analysis on the DEPs across groups by annotating the gene products based on biological processes, cellular components, and molecular functions to discern proteins with significant differences ($P < 0.05$) (**Figure 3A**). Notably, the "granzyme-mediated cell death" and "pyroptosis" of GO terms that are associated with immune downregulation and inflammation relief. Furthermore, to investigate into the pivotal biological processes associated with the DEPs in the tissues, we performed KEGG pathway enrichment analysis (**Figure 3C**). The "Mucin type O-glycan biosynthesis ($P = 4.43E-05$)" may be related to barrier function.

L-sodium lactate activates pro-proliferative and migratory programs in colorectal cancer cell lines

Given the prominent activation of proliferation-related pathways and up-regulation of proteins such as PCNA observed in our proteomic analysis, we next aimed to validate the direct effect of L-sodium lactate on intestinal cell proliferation *in vitro*. CCK-8 assay showed that 10 μM L-sodium lactate significantly enhanced proliferation in MC38 cells compared to the control ($P < 0.05$), whereas the same treatment did not produce a significant effect in HCT116 cells ($P > 0.05$). In contrast, 100 μM L-sodium lactate showed no significant effect on either cell (**Figure 4A** and **4F**). This pro-proliferative effect was further confirmed by colony formation assay, with both cells forming significantly more colonies in the 10 μM group than in the control ($P < 0.05$). Moreover, in wound healing assays, 10 μM L-sodium lactate significantly accelerated wound closure in both MC38 and HCT116 cells at 24 h ($P < 0.05$), while 100 μM had no effect on migration speed ($P > 0.05$), consis-

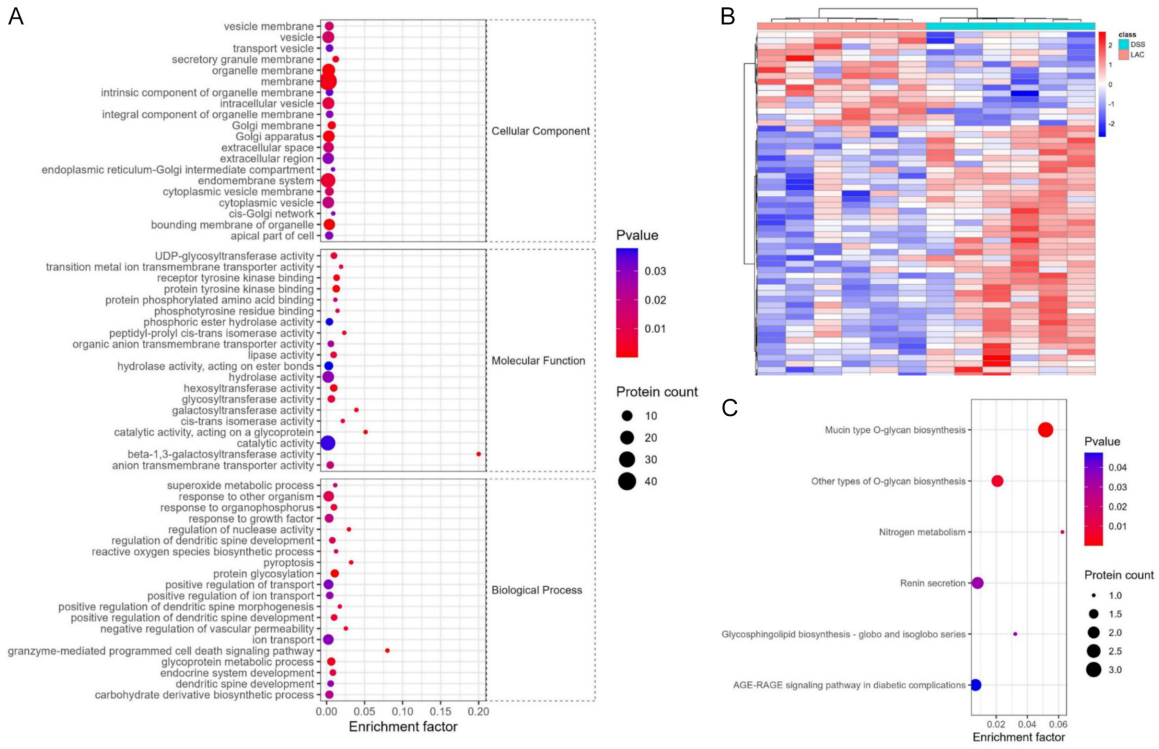

Figure 3. Functional profiling of the L-sodium lactate-responsive proteome identifies key pathways in colitis of mice. A: Gene ontology (GO) functional enrichment analysis of differentially expressed proteins (DEPs); B: Hierarchical clustering diagram of differentially expressed proteins (DEPs); C: Kyoto Encyclopedia of Genes and Genomes (KEGG) Pathway Enrichment Bubble Plot.

tent with the proliferation data (**Figure 4B-E**, **4G-J**).

L-sodium lactate stimulates proliferative-related signaling pathways in vitro

To investigate the molecular mechanisms underlying the pro-proliferative effects observed in functional assays, we analyzed the expression of c-Myc (a key regulator of cell growth) and PCNA (a DNA replication marker) by Western blot given their established roles in cell cycle progression. Preliminary experiments indicated that 100 μM L-sodium lactate did not significantly alter cell proliferation (data not shown). Consequently, both MC38 and HCT116 cells were divided into Ctrl and 10 μM groups. As shown in **Figure 5A-F**, both c-Myc and PCNA proteins expression levels were significantly upregulated in the 10 μM group compared to the Ctrl group ($P < 0.05$).

Discussion

Currently, the clinical management of IBD is chiefly concerned with the utilization of anti-inflammatory medications and immunosuppressive agents, including corticosteroids, azathioprine and 5-aminosalicylic acid [33, 34]. Nevertheless, in view of the potential adverse effects associated with these medications, it is urgent to explore safer and more effective therapeutic strategies [35-39]. L-sodium lactate, as a specific substrate, could potentially mediate histone lactylation and transcriptionally regulate genes such as Arginase 1 (Arg1), thereby promoting the conversion of M1 macrophages to the M2 phenotype and exerting anti-inflammatory effects [40-45]. However, this remains to be validated in future studies measuring macrophage markers (e.g., iNOS, Arg1, CD206) directly in our model. DSS-induced intestinal inflammation predominantly affects colonic tissues, and manifests pathologically through reduced colon length and altered serum inflammatory factors [46, 47]. In this study, colon length measurements in mice demonstrated a significantly greater length in the LAC group when compared with the DSS group. Moreover, the serum IL-10 concentration was found to be significantly higher in mice from the LAC group

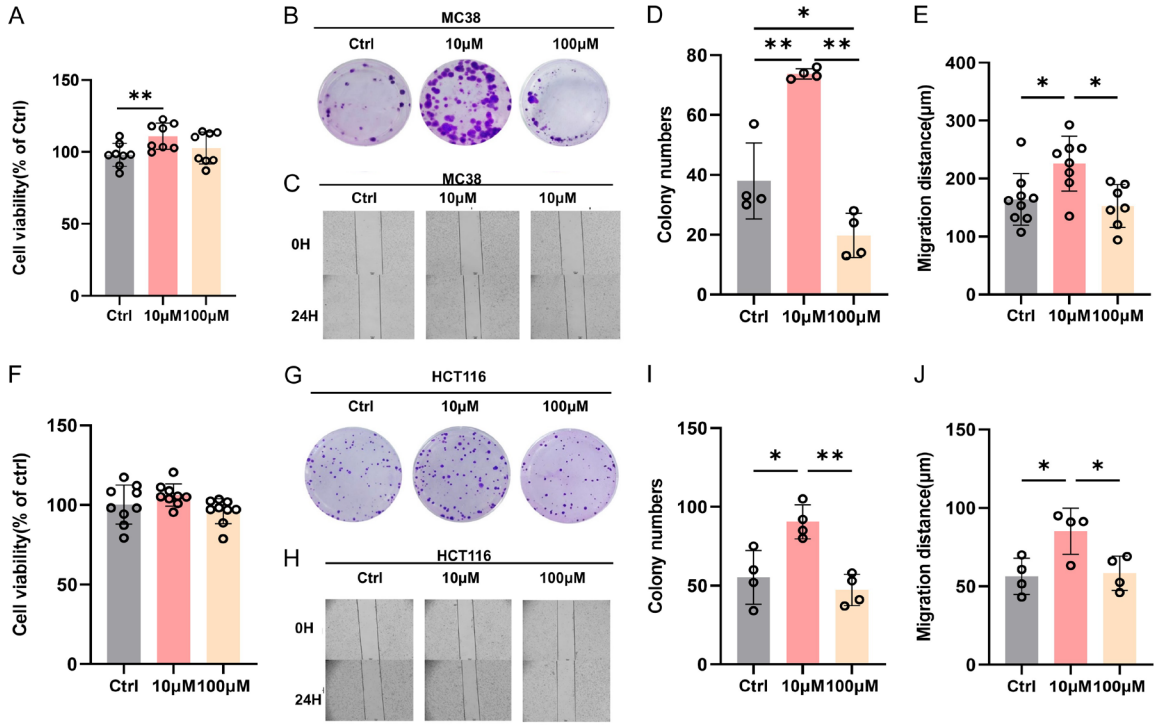

Figure 4. Effects of L-Sodium Lactate on proliferation and migration of MC38 and HCT116 cells. A: MC38 cell viability changes; B: Colony formation assay on MC38; C: MC38 wound healing assay; D: MC38 colony number changes; E: MC38 migration distance changes; F: HCT116 cell viability changes; G: Colony formation assay on HCT116; H: HCT116 wound healing assay; I: HCT116 colony number changes; J: HCT116 migration distance changes. *P < 0.05, **P < 0.01, ***P < 0.001. Scale bar = 100 μm.

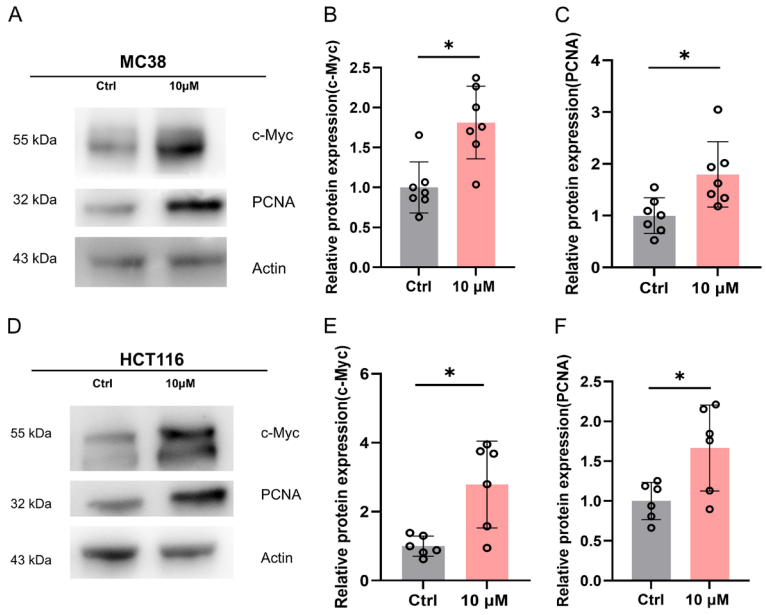

Figure 5. Western blot analysis of c-Myc and PCNA protein expression *in vitro*. A: MC38 western blot analysis of c-Myc and PCNA expression; B: MC38 c-Myc expression changes; C: MC38 PCNA expression changes; D: HCT116 western blot analysis of c-Myc and PCNA expression; E: HCT116 c-Myc expression changes; F: HCT116 PCNA expression changes. *P < 0.05, **P < 0.01, ***P < 0.001.

than in those from the DSS group. These results collectively indicated that L-lactate may alleviate DSS-induced colitis by preserving colon morphology and modulating M1 macrophage polarization. While these findings suggest that L-sodium lactate may promote epithelial repair, the use of cancer cell lines limits direct extrapolation to normal epithelium. Future studies should employ normal intestinal epithelial models to assess therapeutic safety, particularly given the increased colorectal cancer risk in IBD.

We conducted a study on the DEPs in the proteomics results, mitochondria-related functional protein Mfn1, a protein involved in mitochondrial

fusion was identified. After being taken up by the intestinal epithelium, L-sodium lactate can be converted into pyruvate and enter mitochondria, thereby indirectly upregulating the expression of Mitofusin-1 [48]. Also, the SMC protein was up-regulated in the colitis mouse colon after treatment with L-sodium lactate and is essential for chromosomal structure maintenance and segregation, while it engages in DNA organization, condensation, and repair to safeguard the precise transmission of genetic information [49]. Conversely, L-sodium lactate has been observed to down-regulate immune-related proteins (e.g., Immunoglobulin variants, Granzyme A) and signaling regulators (e.g., GR, PPIase, B3GALT5), thereby attenuating inflammatory cascades [50-52]. Notably, KEGG analysis indicated that the most significant pathway is Mucin type O-glycan biosynthesis enriched with down-regulated proteins (e.g., Beta-1,3-galactosyl-O-glycosyl-glycoprotein).

In addition, proteomics results showed an up-regulation of PCNA. The PCNA acts as the sliding clamp for DNA polymerase δ, which is integral to DNA replication and repair, and serves as a significant marker for cell cycle regulation [53]. c-Myc is located upstream of PCNA and serves as a key transcription factor regulating the cell cycle [54]. L-sodium lactate sodium at a certain concentration can promote cell proliferation and migration, and up-regulate the protein expression of c-Myc and PCNA *in vitro*, suggesting that L-sodium lactate treatment may stimulate cell proliferation through the c-Myc/PCNA signaling pathway. It should be noted that the in vitro proliferation and migration assays were performed in colorectal cancer cell lines (MC38/HCT116), which may not fully represent normal intestinal epithelial behavior. Future studies using non-transformed intestinal epithelial cells or organoids will be necessary to validate the physiological relevance of these findings. Additionally, the absence of a healthy control group in the proteomic analysis limits the ability to distinguish DSS-specific effects from L-sodium lactate-mediated changes, a point that should be addressed in future work.

Conclusion

Overall, this study combines disease phenotypic observations *in vivo*, proteomic screening, and functional validation *in vitro* to demonstrate that L-sodium lactate may help alleviate colitis by modulating the immune response and promoting epithelial regeneration. However, the underlying mechanisms require further investigation.

Acknowledgements

We gratefully acknowledge the support of the Institutional Research Grant of Zhenjiang First People's Hospital (Grant No. Y2025001-JDLCYJS).

Disclosure of conflict of interest

None.

Address correspondence to: Zheng-Rong Zhou, School of Medicine, Jiangsu University, Zhenjiang 212013, Jiangsu, PR China. E-mail: zrzhou@ujs.edu.cn

References

[1] Kaplan GG and Ng SC. Understanding and preventing the global increase of inflammatory bowel disease. Gastroenterology 2017; 152: 313-321, e312.

[2] Ng SC, Shi HY, Hamidi N, Underwood FE, Tang W, Benchimol EI, Panaccione R, Ghosh S, Wu JCY, Chan FKL, Sung JJY and Kaplan GG. Worldwide incidence and prevalence of inflammatory bowel disease in the 21st century: a systematic review of population-based studies. Lancet 2017; 390: 2769-2778.

[3] Chen Y, Liang J, Chen S, Lin N, Xu S, Miao J, Zhang J, Chen C, Yuan X, Xie Z, Zhu E, Cai M, Wei X, Hou S and Tang H. Discovery of vitexin as a novel VDR agonist that mitigates the transition from chronic intestinal inflammation to colorectal cancer. Mol Cancer 2024; 23: 196.

[4] Cassotta M, Cianciosi D, De Giuseppe R, Navarro-Hortal MD, Armas Diaz Y, Forbes-Hernández TY, Pifarre KT, Pascual Barrera AE, Grosso G, Xiao J, Battino M and Giampieri F. Possible role of nutrition in the prevention of inflammatory bowel disease-related colorectal cancer: a focus on human studies. Nutrition 2023; 110: 111980.

[5] Ananthakrishnan AN, Bernstein CN, Iliopoulos D, Macpherson A, Neurath MF, Ali RAR, Vavricka SR and Fiocchi C. Environmental triggers in IBD: a review of progress and evidence. Nat Rev Gastroenterol Hepatol 2018; 15: 39-49.

[6] Pan YJ, Lin MC, Liou JM, Fan CC, Su MH, Chen CY, Wu CS, Chen PC, Huang YT and Wang SH. A population-based study of familial coaggregation and shared genetic etiology of psychiatric and gastrointestinal disorders. Commun Med (Lond) 2024; 4: 180.

[7] Mentella MC, Scaldaferri F, Pizzoferrato M, Gasbarrini A and Miggiano GAD. Nutrition, IBD and gut microbiota: a review. Nutrients 2020; 12: 944.
[8] Zhou M, Liu X, He J, Xu X, Ju C, Luo S, Lu X, Du P and Chen Y. High-fructose corn syrup aggravates colitis via microbiota dysbiosis-mediated Th17/Treg imbalance. Clin Sci (Lond) 2023; 137: 1619-1635.
[9] Huang P, Wang X, Wang S, Wu Z, Zhou Z, Shao G, Ren C, Kuang M, Zhou Y, Jiang A, Tang W, Miao J, Qian X, Gong A and Xu M. Treatment of inflammatory bowel disease: potential effect of NMN on intestinal barrier and gut microbiota. Curr Res Food Sci 2022; 5: 1403-1411.
[10] Vich Vila A, Zhang J, Liu M, Faber KN and Weersma RK. Untargeted faecal metabolomics for the discovery of biomarkers and treatment targets for inflammatory bowel diseases. Gut 2024; 73: 1909-1920.
[11] Santoru ML, Piras C, Murgia F, Leoni VP, Spada M, Murgia A, Liggi S, Lai MA, Usai P, Caboni P, Manzin A and Atzori L. Metabolic alteration in plasma and biopsies from patients with IBD. Inflamm Bowel Dis 2021; 27: 1335-1345.
[12] Li J, Ma P, Liu Z and Xie J. L- and D-Lactate: unveiling their hidden functions in disease and health. Cell Commun Signal 2025; 23: 134.
[13] Nasu Y, Murphy-Royal C, Wen Y, Haidey JN, Molina RS, Aggarwal A, Zhang S, Kamijo Y, Paquet ME, Podgorski K, Drobizhev M, Bains JS, Lemieux MJ, Gordon GR and Campbell RE. A genetically encoded fluorescent biosensor for extracellular L-lactate. Nat Commun 2021; 12: 7058.
[14] Young A, Oldford C and Mailloux RJ. Lactate dehydrogenase supports lactate oxidation in mitochondria isolated from different mouse tissues. Redox Biol 2020; 28: 101339.
[15] Adeva M, González-Lucán M, Seco M and Donapetry C. Enzymes involved in l-lactate metabolism in humans. Mitochondrion 2013; 13: 615-629.
[16] Htyte N, White L, Sandhu G, Jones J and Meisels I. An extreme and life-threatening case of recurrent D-lactate encephalopathy. Nephrol Dial Transplant 2011; 26: 1432-1435.
[17] Jin S, Chen X, Yang J and Ding J. Lactate dehydrogenase D is a general dehydrogenase for D-2-hydroxyacids and is associated with D-lactic acidosis. Nat Commun 2023; 14: 6638.
[18] Petersen C. D-lactic acidosis. Nutr Clin Pract 2005; 20: 634-645.
[19] Wu Y, Dong Y, Atefi M, Liu Y, Elshimali Y and Vadgama JV. Lactate, a neglected factor for diabetes and cancer interaction. Mediators Inflamm 2016; 2016: 6456018.
[20] Wu P, Zhu T, Huang Y, Fang Z and Luo F. Current understanding of the contribution of lactate to the cardiovascular system and its therapeutic relevance. Front Endocrinol (Lausanne) 2023; 14: 1205442.
[21] San-Millán I and Brooks GA. Assessment of metabolic flexibility by means of measuring blood lactate, fat, and carbohydrate oxidation responses to exercise in professional endurance athletes and less-fit individuals. Sports Med 2018; 48: 467-479.
[22] Fang Y, Li Z, Yang L, Li W, Wang Y, Kong Z, Miao J, Chen Y, Bian Y and Zeng L. Emerging roles of lactate in acute and chronic inflammation. Cell Commun Signal 2024; 22: 276.
[23] Wang D, Gao Q, Zhao G, Kan Z, Wang X, Wang H, Huang J, Wang T, Qian F, Ho CT and Wang Y. Protective effect and mechanism of theanine on lipopolysaccharide-induced inflammation and acute liver injury in mice. J Agric Food Chem 2018; 66: 7674-7683.
[24] Zhou J, Hu X, Zhang N, Chu Y, Wang J, Cui X, Zhang Y, Han R, Liu C, Yang S and Li J. Proteomic analysis reveals differential protein expression in placental tissues of early-onset preeclampsia patients. J Proteome Res 2024; 23: 4433-4442.
[25] Yang Q, Zhang X, Solairaj D, Lin R, Wang K and Zhang H. TMT-based proteomic analysis of hannaella sinensis-induced apple resistance-related proteins. Foods 2023; 12: 2637.
[26] Wang YY, Yan JK, Ding Y and Ma H. Effects of ultrasound on the thawing of quick-frozen small yellow croaker (Larimichthys polyactis) based on TMT-labeled quantitative proteomic. Food Chem 2022; 366: 130600.
[27] Yu XT, Wang F, Ding JT, Cai B, Xing JJ, Guo GH and Guo F. Tandem mass tag-based serum proteomic profiling revealed diabetic foot ulcer pathogenesis and potential therapeutic targets. Bioengineered 2022; 13: 3171-3182.
[28] Mao X, Yang S, Zhang Y, Yang H, Yan D and Zhang L. The role of chromatin modulator DPY30 in glucose metabolism of colorectal cancer cells. Transl Cancer Res 2024; 13: 4205-4218.
[29] Xia T, Duan W, Zhang Z, Fang B, Zhang B, Xu B, de la Cruz CBV, El-Seedi H, Simal-Gandara J, Wang S, Wang M and Xiao J. Polyphenol-rich extract of Zhenjiang aromatic vinegar ameliorates high glucose-induced insulin resistance by regulating JNK-IRS-1 and PI3K/Akt signaling pathways. Food Chem 2021; 335: 127513.
[30] Wang J, Shi L, Zhang X, Hu R, Yue Z, Zou H, Peng Q, Jiang Y and Wang Z. Metabolomics and proteomics insights into subacute ruminal acidosis etiology and inhibition of proliferation

of yak rumen epithelial cells in vitro. BMC Genomics 2024; 25: 394.
[31] Ma J, Chen T, Wu S, Yang C, Bai M, Shu K, Li K, Zhang G, Jin Z, He F, Hermjakob H and Zhu Y. iProX: an integrated proteome resource. Nucleic Acids Res 2019; 47: D1211-D1217.
[32] Chen T, Ma J, Liu Y, Chen Z, Xiao N, Lu Y, Fu Y, Yang C, Li M, Wu S, Wang X, Li D, He F, Hermjakob H and Zhu Y. iProX in 2021: connecting proteomics data sharing with big data. Nucleic Acids Res 2022; 50: D1522-D1527.
[33] Neurath MF. Current and emerging therapeutic targets for IBD. Nat Rev Gastroenterol Hepatol 2017; 14: 269-278.
[34] Pithadia AB and Jain S. Treatment of inflammatory bowel disease (IBD). Pharmacol Rep 2011; 63: 629-642.
[35] Kochar B, Cai W, Cagan A and Ananthakrishnan AN. Pretreatment frailty is independently associated with increased risk of infections after immunosuppression in patients with inflammatory bowel diseases. Gastroenterology 2020; 158: 2104-2111, e2102.
[36] Hasan S, Ghani N, Zhao X, Good J and Liu CJ. Exogenous pyruvate is therapeutic against colitis by targeting cytosolic phospholipase A2. Genes Dis 2025; 12: 101571.
[37] Chang CL, Chen CH, Chen YL, Chiang JY, Wang YT, Huang CR, Chen HH and Yip HK. Synergic effect of combined melatonin and tofacitinib on ameliorating dextran sulfate sodium-induced colitis in rat--role of JAKs/STAT, cell-stress signaling, and inflammatory-immune reaction. Am J Clin Exp Immunol 2025; 14: 185-203.
[38] Michaudel C, Danne C, Agus A, Magniez A, Aucouturier A, Spatz M, Lefevre A, Kirchgesner J, Rolhion N, Wang Y, Lavelle A, Galbert C, Da Costa G, Poirier M, Lapière A, Planchais J, Nádvorník P, Illes P, Oeuvray C, Creusot L, Michel ML, Benech N, Bourrier A, Nion-Larmurier I, Landman C, Richard ML, Emond P, Seksik P, Beaugerie L, Arguello RR, Moulin D, Mani S, Dvorák Z, Bermúdez-Humarán LG, Langella P and Sokol H. Rewiring the altered tryptophan metabolism as a novel therapeutic strategy in inflammatory bowel diseases. Gut 2023; 72: 1296-1307.
[39] Xu J, Li J, Guo X, Huang C, Peng Y, Xu H, Li Y, Xu J, Hu J, Liao Y, Nie Y and Zhou Y. Secondary bile acids modified by odoribacter splanchnicus alleviate colitis by suppressing neutrophil extracellular trap formation. Adv Sci (Weinh) 2025; 12: e09073.
[40] Ma F, Zhang S, Akanyibah FA, Zhang W, Chen K, Ocansey DKW, Lyu C and Mao F. Exosome-mediated macrophage regulation for inflammatory bowel disease repair: a potential target of gut inflammation. Am J Transl Res 2023; 15: 6970-6987.
[41] Zhang J, Muri J, Fitzgerald G, Gorski T, Gianni-Barrera R, Masschelein E, D'Hulst G, Gilardoni P, Turiel G, Fan Z, Wang T, Planque M, Carmeliet P, Pellerin L, Wolfrum C, Fendt SM, Banfi A, Stockmann C, Soro-Arnáiz I, Kopf M and De Bock K. Endothelial lactate controls muscle regeneration from ischemia by inducing M2-like macrophage polarization. Cell Metab 2020; 31: 1136-1153, e1137.
[42] Rong Y, Dong F, Zhang G, Tang M, Zhao X, Zhang Y, Tao P and Cai H. The crosstalking of lactate-Histone lactylation and tumor. Proteomics Clin Appl 2023; 17: e2200102.
[43] Chen AN, Luo Y, Yang YH, Fu JT, Geng XM, Shi JP and Yang J. Lactylation, a novel metabolic reprogramming code: current status and prospects. Front Immunol 2021; 12: 688910.
[44] Yang K, Fan M, Wang X, Xu J, Wang Y, Tu F, Gill PS, Ha T, Liu L, Williams DL and Li C. Lactate promotes macrophage HMGB1 lactylation, acetylation, and exosomal release in polymicrobial sepsis. Cell Death Differ 2022; 29: 133-146.
[45] Wang N, Wang W, Wang X, Mang G, Chen J, Yan X, Tong Z, Yang Q, Wang M, Chen L, Sun P, Yang Y, Cui J, Yang M, Zhang Y, Wang D, Wu J, Zhang M and Yu B. Histone lactylation boosts reparative gene activation post-myocardial infarction. Circ Res 2022; 131: 893-908.
[46] Li X, Zhang ZH, Zabed HM, Yun J, Zhang G and Qi X. An insight into the roles of dietary tryptophan and its metabolites in intestinal inflammation and inflammatory bowel disease. Mol Nutr Food Res 2021; 65: e2000461.
[47] Liang Q, Ren X, Chalamaiah M and Ma H. Simulated gastrointestinal digests of corn protein hydrolysate alleviate inflammation in caco-2 cells and a mouse model of colitis. J Food Sci Technol 2020; 57: 2079-2088.
[48] Park YY and Cho H. Mitofusin 1 is degraded at G2/M phase through ubiquitylation by MARCH5. Cell Div 2012; 7: 25.
[49] Jeppsson K, Kanno T, Shirahige K and Sjögren C. The maintenance of chromosome structure: positioning and functioning of SMC complexes. Nat Rev Mol Cell Biol 2014; 15: 601-614.
[50] Proud CG. Regulation and roles of elongation factor 2 kinase. Biochem Soc Trans 2015; 43: 328-332.
[51] Yang X, Geng J and Meng H. Glucocorticoid receptor modulates dendritic cell function in ulcerative colitis. Histol Histopathol 2020; 35: 1379-1389.
[52] Huang Y, Gao Y, Lin Z and Miao H. Involvement of the ubiquitin-proteasome system in the reg-

ulation of the tumor microenvironment and progression. Genes Dis 2024; 12: 101240.
[53] Simonsen S, Søgaard CK, Olsen JG, Otterlei M and Kragelund BB. The bacterial DNA sliding clamp, β-clamp: structure, interactions, dynamics and drug discovery. Cell Mol Life Sci 2024; 81: 245.
[54] Duan Y, Liu Z, Wang Q, Zhang J, Liu J, Zhang Z and Li C. Targeting MYC: multidimensional regulation and therapeutic strategies in oncology. Genes Dis 2024; 12: 101435.

Table S1. Western blot antibodies

Antibody	Brand	Cat	Lot
β-actin Rabbit mAb	AiFang biological	AFRM9010	ZJDZ250215
PCNA Rabbit mAb	AiFang biological	AFRM9141	ZJDZ250215
c-Myc Antibody	AiFang biological	AFRM80201	ZJDZ250415
HRP Conjugated Goat Anti-Rabbit IgG(H+L)	AiFang biological	AFSA004	ZJDZ250215